Available online at www.sciencedirect.com
SCIENCE DIRECT®
ELSEVIER
Journal of Solid State Chemistry 179 (2006) 3–17
JOURNAL OF SOLID STATE CHEMISTRY
www.elsevier.com/locate/jssc

New open-framework three-dimensional lanthanide oxalates containing as a template the diprotonated 1,2- or 1,3-diaminopropane

A. Mohanu, C. Brouca-Cabarrecq, J.C. Trombe*

CEMES/CNRS, 29 rue J. Marvig, BP 94347, 31055 Toulouse Cedex 4, France

Received 21 March 2005; received in revised form 13 September 2005; accepted 17 September 2005
Available online 27 October 2005

Abstract

Single crystals of three new open-framework lanthanide oxalates have been synthesized hydrothermally, in the presence of 1,2-diaminopropane, $(C_3N_2H_{12})[Nd(H_2O)(C_2O_4)_2]_2 \cdot 3H_2O$ **I** and $(C_3N_2H_{12})[Yb(C_2O_4)_2]_2 \cdot 5H_2O$ **II**, or 1,3-diaminopropane $(C_3N_2H_{12})_2[La_2(C_2O_4)_5] \cdot 5H_2O$ **III**. Their structures have been determined by X-ray diffraction data: **I** and **III** crystallize in the triclinic system, space group *P*-1, with $a = 7.8130(5)$ Å, $b = 11.8800(6)$ Å, $c = 12.9940(8)$ Å, $\alpha = 93.092(5)^\circ$, $\beta = 93.930(6)^\circ$, $\gamma = 108.359(5)^\circ$ and $a = 11.6650(9)$ Å, $b = 11.9240(6)$ Å, $c = 13.2230(7)$ Å, $\alpha = 104.585(4)^\circ$, $\beta = 108.268(5)^\circ$, $\gamma = 111.132(5)^\circ$, respectively while **II** crystallizes in the orthorhombic system, space group *F2dd*, with $a = 8.7970(4)$ Å, $b = 16.1550(8)$ Å, $c = 32.170(2)$ Å. The three-dimensional (3D) framework of these compounds is built up by the linkages of lanthanide atoms and the oxygen atoms of the bischelating oxalate ligands. Instead of four chelating oxalate units surrounding a lanthanide atom (**I** and **II**), both lanthanum atoms, in **III**, are surrounded by five chelating oxalate groups and that is new. In all the cases within the frame, are observed 8- and 12-membered channels where are localized the guest species, 1,2- or 1,3-diaminopropane cations and free water molecules. The ratio of the guest number (especially the diaminopropane) per 12-membered ring could tune the shape and the size of 12-membered channels: thus, the 12-membered channels, observed for **I** and **II**, have elliptical cross-section (5.5 Å × 11.4 Å and 5.2 Å × 9.5 Å) while those, observed for **III**, have nearly circular cross-section (9.1 Å × 9.5 Å). The lanthanide atoms are 8, 9 and 10-fold coordinated for Yb (**II**), Nd (**I**) and La (**III**), respectively.

Keywords: Lanthanide; Oxalate; Template; Open-structure

---

1. Introduction

In the last few years, a great number of organically templated open-framework compounds have been synthesized especially using the hydrothermal route [1–16]. The chemistry of hybrid materials has been widely developed, as well. The organic multi-functional ligand acts as a spacer between the metals to build up materials of which the porosity depends essentially on the size, shape and geometry of both the spacer and the template ligands. Several structural agents have been used in these syntheses leading to various structural types.

For our part, we have been particularly interested in lanthanide oxalates [17–19]. Except for the three-dimensional (3D), $[\{Er(H_2O)_3\}_2(C_2O_4)_3] \cdot 12H_2O$, whose the structure was solved recently [20], these oxalates present a layered honey-comb open-architecture, whether they are decahydrates or hexahydrates [21–24]. Mixed oxalates, lanthanide-alkaline element (including ammonium), are either bi-dimensional [25–29] or tri-dimensional [30,31].

When synthesized hydrothermally in presence of an organic template, their structure is bi-dimensional or 3D:

- Only layers are found in $(NH_4)(CN_3H_6)[Nd(H_2O)(C_2O_4)_2]_2$ or $(CN_3H_6)[La(H_2O)(C_2O_4)_2]$ [32]. In the former example, the ammonium ion was not present as a starting reagent, but it comes from partial hydrolysis of the guanidinium ion in the synthesis conditions.
- The guanidinium can also lead to a 3D open structure, $(CN_3H_6)_2[Ln(H_2O)(C_2O_4)_2]_2 \cdot 3H_2O$ with $Ln = $ La…Eu,

---

*Corresponding author. Fax: +33 5 62 25 79 99.
E-mail address: trombe@cemes.fr (J.C. Trombe).

0022-4596/$ - see front matter © 2005 Elsevier Inc. All rights reserved.
doi:10.1016/j.jssc.2005.09.044

as well as tetramethylammonium ion [33,34]. However as reported by Vaidhyanathan et al., 1,2-diaminopropane (1,2DAP) or 1,3-diaminopropane (1,3DAP) can condensate with some acids to give rise to more complex protonated amines [35,36]. A nice example of such reaction is the formation of *N*-(2-aminopropyl acetamide), by reacting 1,2DAP with acetic acid, in the used hydrothermal conditions [36]. One part of this latter group is dangling about the neodymium atom via the oxygen of acetamide but the other part is protruding into 12-membered channels, similar to guanidinium or tetramethylammonium ions in the examples quoted before [33,34].

Considering the tendency of 1,2DAP or 1,3DAP to give more complex amines, we have also tried to use such templates, in the formation of lanthanide oxalates using mild hydrothermal synthesis. In this way, we successfully isolated three 3D open-framework lanthanide oxalates containing the diprotonated 1,2DAP, $(C_3N_2H_{12})[Nd(H_2O)(C_2O_4)_2]_2 \cdot 3H_2O$ **I** and $(C_3N_2H_{12})[Yb(C_2O_4)_2]_2 \cdot 5H_2O$ **II** or 1,3DAP ions, $(C_3N_2H_{12})_2[La_2(C_2O_4)_5] \cdot 5H_2O$ **III**. The above compounds will be compared to each other and to those reported in the literature. An extension of the compound **I** to some other lanthanide elements is realized, leading to a family with $Ln = \text{Ce}\ldots\text{Tm}$. At last, a characterization by infrared spectroscopy and thermogravimetric analysis has been carried out on some of these pure compounds.

2. Experimental part

2.1. Synthesis

The three compounds were synthesized hydrothermally (autogenous pressure) using 1,2DAP for the first two and

Table 1
Experimental crystallographic data for $(C_3N_2H_{12})[Nd(H_2O)(C_2O_4)_2]_2 \cdot 3H_2O$ **I**, $(C_3N_2H_{12})[Yb(C_2O_4)_2]_2 \cdot 5H_2O$ **II** and $(C_3N_2H_{12})_2[La_2(C_2O_4)_5] \cdot 5H_2O$ **III**

Crystal data	**I**	**II**	**III**
System	Triclinic	Orthorhombic	Triclinic
Space group	*P*-1 (2)	*F*2*dd* (43)	*P*-1 (2)
a (Å)	7.8130(5)	8.7970(4)	11.6650(9)
b (Å)	11.8800(6)	16.1550(8)	11.9240(6)
c (Å)	12.9940(8)	32.170(2)	13.2230(7)
α (deg)	93.092(5)	90	104.585(4)
β (deg)	93.930(6)	90	108.268(5)
γ (deg)	108.359(5)	90	111.132(5)
V (Å^3)	1138.3(1)	4571.9(4)	1484.5(2)
Molecular weight (g mol^{-1})	806.79	864.39	960.29
Z/formula	2	8	2
ρ_{cal} (g cm^{-3})	2.354	2.512	2.148
μ(Mo*K*α) (cm^{-1})	46.14	82.35	29.50
Transmission	Min = 0.408	Min = 0.386	Min = 0.317
Coefficient range	Max = 0.758	Max = 0.449	Max = 0.820
Morphology	Parallepipedic	Octahedron	Parallepipedic
Crystal size (mm)	0.12 × 0.11 × 0.06	0.09 × 0.07 × 0.06	0.12 × 0.11 × 0.06
Color	Pale blue	Colorless	Colorless
Data collection			
Temperature (°C)	20	20	20
Wavelength Mo(*K*α) (Å)	0.71073	0.71073	0.71073
Monochromator	Graphite	Graphite	Graphite
Max. Bragg angle (deg)	30	29.95	30
Data collected	$-10 \leqslant h \leqslant 10$	$-9 \leqslant h \leqslant 12$	$-16 \leqslant h \leqslant 15$
	$-13 \leqslant k \leqslant 16$	$-17 \leqslant \mathrm{k} \leqslant 22$	$-16 \leqslant k \leqslant 16$
	$-21 \leqslant l \leqslant 21$	$-38 \leqslant \mathrm{l} \leqslant 45$	$-18 \leqslant l \leqslant 18$
Structure refinement			
Flack parameter		−0.005(15)	
No. unique data	6008	3081	8509
No. data ($I \geqslant 2\sigma$(I))_obs.	4290	2675	4778
No. refined parameters	286	140	350
*R*_obs. %	3.61	3.03	6.27
wR_obs. %	8.59	5.63	15.06
S	1.040	1.001	0.958
Weighting scheme[a]	0.0371/3.0980	0.0269/0.0000	0.0951/0.0000
$(\Delta/\sigma)_{max}$	0.001	0.001	0.000
$(\Delta/\rho)_{max}$	2.215	1.603	3.534
$(\Delta/\rho)_{min}$	−1.714	−0.952	−3.136

[a] $w = 1/[\sigma^2(F_o^2) + (aP)^2 + bP]$, $P = [(F_o^2) + 2(F_c)^2]/3$.

Table 2
Final least-squares atomic parameters with estimated standard deviations for $(C_3N_2H_{12})[Nd(H_2O)(C_2O_4)_2]_2 \cdot 3H_2O$ **I**

Atoms	x	y	z	$U_{eq.}$ (Å)^2
Nd1	0.15004(3)	0.77776(2)	0.03190(2)	0.01639(9)
Nd2	0.15651(3)	0.78215(2)	0.53207(2)	0.01532(9)
O1	−0.0153(5)	0.7271(4)	0.3578(3)	0.0313(9)
O2	−0.0177(5)	0.7188(3)	0.1868(2)	0.0254(8)
O3	0.3412(5)	0.8254(3)	0.2036(2)	0.0229(7)
O4	0.3446(5)	0.8216(3)	0.3765(2)	0.0226(7)
O5	0.2117(5)	0.6802(3)	0.6906(3)	0.0304(9)
O6	0.1992(5)	0.6697(3)	0.8615(3)	0.0287(8)
O7	0.1085(6)	0.8733(3)	0.7009(3)	0.0309(9)
O8	0.0813(6)	0.8585(4)	0.8695(3)	0.0328(9)
O9	0.4688(5)	0.8481(3)	−0.0103(3)	0.0270(8)
O10	0.7011(5)	0.9994(3)	−0.0507(3)	0.0231(7)
O11	−0.1152(5)	0.8520(3)	0.5169(3)	0.0247(8)
O12	−0.2220(5)	1.0028(3)	0.4920(3)	0.0244(8)
O13	−0.1118(5)	0.6038(3)	−0.0225(3)	0.0257(8)
O14	−0.2007(5)	0.4087(3)	−0.0693(3)	0.0240(8)
O15	0.2127(5)	0.5956(3)	0.4778(3)	0.0252(8)
O16	0.1095(5)	0.3974(3)	0.4638(3)	0.0267(8)
Ow1	−0.0967(5)	0.8639(3)	0.0510(3)	0.0316(9)
Ow2	0.4834(5)	0.8619(4)	0.5837(3)	0.0342(9)
Ow3	0.7191(6)	0.8746(4)	0.2267(3)	0.040(1)
Ow4	0.7601(7)	0.9332(4)	0.7404(4)	0.055(1)
Ow5	0.5577(9)	0.6263(6)	−0.0008(5)	0.087(2)
C1	0.0598(6)	0.7456(4)	0.2762(4)	0.020(1)
C2	0.2685(6)	0.8044(4)	0.2862(4)	0.019(1)
C3	0.1818(7)	0.7143(5)	0.7783(4)	0.022(1)
C4	0.1184(7)	0.8261(5)	0.7841(4)	0.025(1)
C5	0.5477(6)	0.9551(4)	−0.0173(3)	0.0180(9)
C6	−0.0974(6)	0.9572(4)	0.5025(3)	0.0179(9)
C7	−0.0910(6)	0.5036(4)	−0.0264(3)	0.0167(9)
C8	0.0939(7)	0.4978(4)	0.4832(4)	0.019(1)
N1	0.6040(8)	0.6882(5)	0.3797(5)	0.053(1)
N2	0.6489(8)	0.5182(5)	0.1832(4)	0.046(1)
C9	0.487(2)	0.592(1)	0.302(1)	0.109(4)
C10	0.540(1)	0.4975(8)	0.2724(7)	0.072(2)
C11	0.384(1)	0.3850(8)	0.2527(7)	0.068(2)

Table 3
Selected bond distances (Å) and angles (deg) in $(C_3N_2H_{12})[Nd(H_2O)(C_2O_4)_2]_2 \cdot 3H_2O$ **I**

Nd1–O13	2.436(4)	Nd2–Ow2	2.458(4)	
Nd1–O14^{i}	2.438(3)	Nd2–O15	2.468(3)	
Nd1–O8^{ii}	2.460(3)	Nd2–O16^{iv}	2.471(4)	
Nd1–Ow1	2.471(4)	Nd2–O12^{v}	2.484(3)	
Nd1–O9	2.476(3)	Nd2–O1	2.495(3)	
Nd1–O2	2.489(3)	Nd2–O7	2.498(3)	
Nd1–O10^{iii}	2.524(3)	Nd2–O11	2.511(3)	
Nd1–O3	2.530(3)	Nd2–O5	2.525(3)	
Nd1–O6^{ii}	2.611(4)	Nd2–O4	2.557(3)	
O1–C1	1.243(6)	O1–C1–O2	125.7(5)	
O2–C1	1.249(6)	O2–C1–C2	117.1(4)	
O3–C2	1.250(6)	O1–C1–C2	117.2(4)	Ox1
O4–C2	1.255(5)	O3–C2–O4	127.8(5)	
C1–C2	1.551(7)	O3–C2–C1	116.4(4)	
		O4–C2–C1	115.8(4)	
O5–C3	1.250(6)	O6–C3–O5	127.3(5)	
O6–C3	1.247(6)	O6–C3–C4	116.5(4)	
O7–C4	1.253(6)	O5–C3–C4	116.2(4)	Ox2
O8–C4	1.237(6)	O8–C4–O7	126.7(5)	
C3–C4	1.557(7)	O8–C4–C3	117.1(4)	
		O7–C4–C3	116.1(5)	
O9–C5	1.237(5)	O9–C5–O10	126.1(4)	
O10–C5	1.265(6)	O9–C5–C5^{iii}	118.0(5)	Ox3
C5–C5^{iii}	1.546(9)	O10–C5–C5^{iii}	115.9(5)	
O11–C6	1.238(5)	O11–C6–O12	126.6(4)	
O12–C6	1.258(6)	O11–C6–C6^{v}	117.5(5)	Ox4
C6–C6^{v}	1.549(9)	O12–C6–C6^{v}	115.9(5)	
O13–C7	1.249(5)	O13–C7–O14	126.4(4)	
O14–C7	1.255(6)	O13–C7–C7^{i}	116.7(5)	Ox5
C7–C7^{i}	1.565(9)	O14–C7–C7^{i}	116.9(5)	
O15–C8	1.246(6)	O15–C8–O16	126.3(5)	
O16–C8	1.251(6)	O15–C8–C8^{iv}	116.4(5)	Ox6
C8–C8^{iv}	1.57(1)	O16–C8–C8^{iv}	117.3(5)	
Ow1–H1a	0.856	H1a–Ow1–H1b	113.8	
Ow1–H1b	0.930			
Ow2–H2a	0.841	H2a–Ow2–H2b	116.2	
Ow2–H2b	1.000			
Ow3–H3a	1.000	H3a Ow3–H3b	112.1	
Ow3–H3b	0.970			
Ow4–H4a	0.893	H4a–Ow4–H4b	105.7	
Ow4–H4b	0.970			
Ow5–H5a	1.020	H5a–Ow5–H5b	117.8	
Ow5–H5b	1.001			
N1–C9	1.50(1)	C10–C9–N1	121(1)	
N2–C10	1.47(1)	C9–C10–N2	112.8(9)	
C9–C10	1.36(1)	C9–C10–C11	112.6(9)	
C10–C11	1.49(1)	N2–C10–C11	110.7(7)	

Hydrogen bonds and Van der Waals interactions

	D–H	A–H	A–D	D–H–A
Ow1–H1a…O10^{vi}	0.86	2.13	2.893(5)	148.9
Ow1–H1b…Ow3^{vi}	0.93	1.87	2.799(6)	173.6
Ow2–H2a…O12^{vii}	0.84	1.97	2.772(5)	158.0
Ow2–H2b…Ow4	1.00	1.93	2.755(6)	138.2
Ow3–H3a…O3	1.00	1.82	2.814(6)	175.3
Ow3–H3b…O7^{viii}	0.97	1.98	2.942(6)	170.4
Ow4–H4a…O10^{ix}	0.89	2.10	2.893(6)	147.4
Ow4–H4b…O7^{vii}	0.97	2.13	3.090(7)	169.8
Ow5–H5a…O13^{vii}	1.02	1.80	2.711(8)	146.4
Ow5–H5b…O9	1.00	1.97	2.934(8)	159.8
N1–H1c…O4	0.92	2.06	2.939(7)	160.3
N1–H1d…O1^{vii}	0.89	2.21	2.899(7)	134.2
N2–H2c…O6^{x}	0.92	2.01	2.891(7)	160.2
N2–H2d…O2^{vii}	0.91	2.06	2.920(7)	156.8
N2–H2e…Ow5^{xi}	0.89	2.46	2.909(9)	111.8
N2–H2e…Ow5	0.89	2.07	2.924(8)	159.6

Symmetry codes: (i) $-x, 1-y, -z$; (ii) $x, y, z-1$; (iii) $1-x, 2-y, -z$; (iv) $-x, 1-y, 1-z$; (v) $-x, 2-y, 1-z$; (vi) $x-1, y, z$; (vii) $1+x, y, z$; (viii) $1-x, 2-y, 1-z$; (ix) $x, y, 1+z$; (x) $1-x, 1-y, 1-z$; (xi) $1-x, 1-y, -z$; (xii) $x, y-1, z$; (xiii) $-x, 2-y, -z$.

1,3DAP for the third. In a typical synthesis for **I**, 2 mmol of oxalic acid and 1 mmol of 1,2DAP were added to an aqueous suspension (50 mL) of neodyme oxalate (0.5 mmol). For the preparation of **II**, a similar procedure was employed using ytterbium nitrate as the lanthanide source. The Yb/$H_2C_2O_4$/1,2DAP molar ratio was 1/5/2 and the dilution was again 50 mL. For **III**, 6 mmol of oxalic acid and 2 mmol of 1,3DAP were added to an aqueous suspension (10 mL) of lanthanum oxalate decahydrate (0.5 mmol). For the three compounds, this starting mixture was heated at 120 °C for 45, 30 and 14 days for **I**, **II** and **III**, respectively. After cooling down to room temperature, the pH of the final solution was found to be 3.2, 2.0 and 2.9 for **I**, **II** and **III**, respectively. The resulting products, as single crystals, were filtered, washed with distilled water and dried at room temperature.

Powder X-ray analysis was carried out with a Siemens diffractometer using Cu *K*-α radiation. For **I**, the X-ray powder pattern of the bulk sample has been fully indexed on the basis of the unit-cell constants, indicating a pure phase. For **II**, the crystal phase was the major phase of the powder sample, the trace phase was simple ytterbium oxalate hexahydrate. For **III**, a mixture of phases was observed in the powder bulk sample and the crystal phase was the major one, for the moment the other phase(s) remain(s) unknown.

Another route to prepare the compounds **I**–**III**, as a pure phase, consists in refluxing and stirring for some days (2–4) an aqueous suspension (100 mL) of the corresponding lanthanide oxalate, oxalic acid and 1,2DAP or 1,3DAP in a molar ratio 0.5/3/2 or 0.5/5/4.

By varying the lanthanide elements and using 1,2DAP in the first ratio, this last method allowed to extend the family

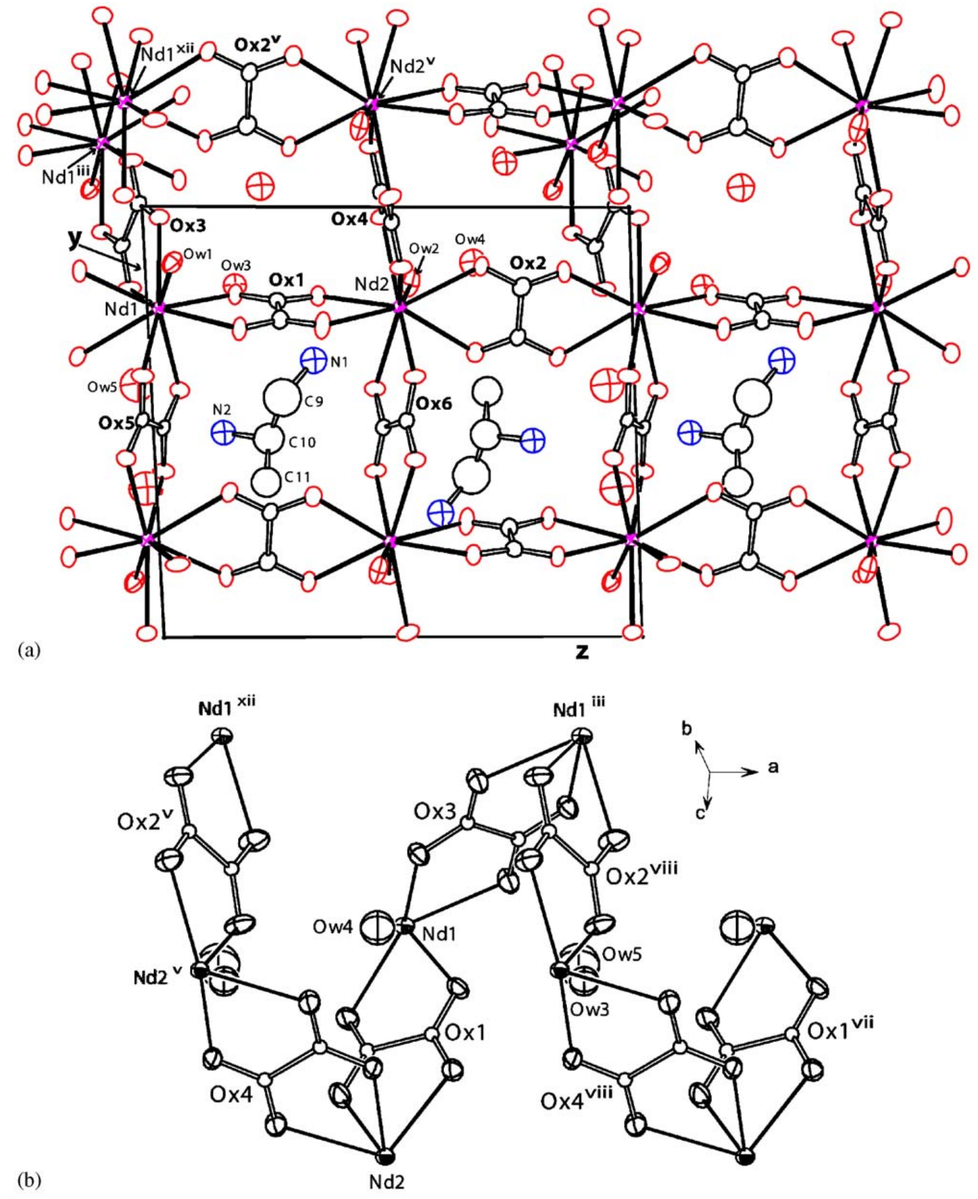

Fig. 1. (a) View, on the (100) plane, of the structure of **I**, showing the 8-membered channels inside the ladder; (b) view of a helix running into the [100] direction (for clarity reason, only the oxygen atoms involved in the helix formation and the free water molecules are drawn). Thermal ellipsoids are represented at 50% probability. The symmetry codes are given in Table 3.

I from Ce to Sm. Using 1,2DAP again, ytterbium, was the only element to present the **II** structure, but it was a pure phase.

Using 1,3DAP, the first ratio did not result in a pure phase of structure **III**. However, the second ratio was successful although limited to only lanthanum. For the other lanthanide elements, this method gave some phase(s) that were characteristic of a family, however we failed to obtain some single crystal representative of this family by the hydrothermal technique.

The study of these families is given after the determination of the structure. Thermogravimetric and DTA analyses of the pure phases (about 20 mg) were performed in the temperature range 20–800 °C, under O_2 flow, at a heating rate of 5 °C/mn by using a Setaram apparatus. Infrared spectra were carried out on a Perkin Elmer 1725 FT-IR spectrometer using a dispersion (about 1.5%) in potassium bromide.

2.2. *Single crystal structure determination*

A single crystal of each compound was carefully selected under a binocular and glued at the tip of a thin fiber. The intensity data of **I**–**III** were collected using a Nonius Kappa CCD four circles diffractometer, with graphite-monochromated Mo-$K\alpha$ ($\lambda = 0.71073$ Å) radiation at room temperature. All the absorption corrections were performed using a multi-scan method [37]. The structures were solved by direct methods [38] and refined on F^2 by a full-matrix least squares using the Shelxl-97 program and difference Fourier synthesis [39]. The hydrogen positions were located in the difference Fourier map and for the final refinement they were refined using the riding mode at their relevant parent atom. For **I**, all the hydrogen were found, for **II** only a part of hydrogen atoms was localized and for **III**, due to the bad quality of the crystal, no hydrogen atoms were found.

For **II**, the 1,2-diaminopropane is disordered. The carbon atom (C5), carrying the nitrogen (N1), was easily found and the distance C5–C5 was 1.56(2) Å. Another peak was localized at a distance of 1.52(2) Å from C5. This site was in a general position like C5 and N1. If this site was totally filled up, the so-obtained template was the 2,3 diaminobutane, but the thermal factors of C5 and C6 were really different, 0.04 and 0.12, respectively. By varying the C6 multiplicity, the obtained value was 0.6 and the U_{iso} of both carbon atoms were quite similar. Hence, the C6 multiplicity was fixed to 1/2, and in that case the obtained organic group is a disordered 1,2-diaminopropane. Such a disordered amine has been observed [35,36,40].

3. Results

3.1. *Description of structures*

The three structures present some similarities and dissimilarities. In all the cases, the 3D network is built up from lanthanide atoms sharing all their oxygen atoms with bischelating oxalates leading, as usually observed in the case of metal-oxalates, to 8- and 12-membered apertures or channels. However, the shape and the size of these apertures, particularly the 12-membered, differ from one structure to the other:

$(C_3N_2H_{12})[Nd(H_2O)\ (C_2O_4)_2]_2 \cdot 3H_2O$ **I**.

The asymmetric unit of **I** contains 36 non-hydrogen atoms of which 28 belong to the frame. Within this latter, there are two independent neodymium atoms, four oxalate ligands (Ox1, Ox2, Ox3, Ox4, Ox5 and Ox6, the four last oxalates being located at the center of symmetry) and two water molecules (Tables 2 and 3). Each neodymium atom is bound to four oxalates and the distances Nd–Nd through these oxalates are in the range 6.2557(5) Å (via Ox5) to 6.5013(5) Å (via Ox2).

The connectivity between Nd1 and Nd2 and oxalate units, Ox1, Ox2, Ox5 and Ox6 forms a ladder running in the [001] direction (Fig. 1a). The uprights of this ladder consist of two independent Nd atoms and the two first oxalates (Ox1 and Ox2) in an alternative manner, the dihedral angle between these last oxalates being 78.8(1)°. Ox5 and Ox6 units act as rungs also in alternative manner. This ladder define some 8-membered channels (4.6 Å × 5.3 Å). The dimensions, given here, are roughly the average distances of the shortest oxygen atoms (i.e. the narrowest space or "bottleneck"), that are the wall of this aperture or channel, including the Van der Waals radii (the same remark applies to all aperture size observed here). The diprotonated 1,2DAP is localized below or above the level of this 8-membered channel. One supplementary oxalate, Ox4, interconnects these ladders leading to a corrugated layer parallel to the (100) plane. However, Ox3 bridges these ladders again, in out-of-plane manner or by translating the *x* coordinate (−1 or +1). In fact, the frame displayed by Ox3, Ox1, Ox4 and Ox2$^{\text{v}}$ is a helix spreading

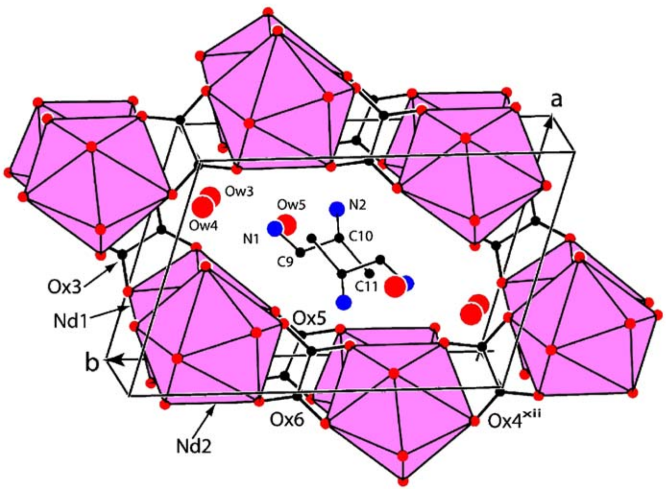

Fig. 2. View of the 12-membered channel, spreading into the [001] direction, for **I**. The symmetry codes are given in Table 3.

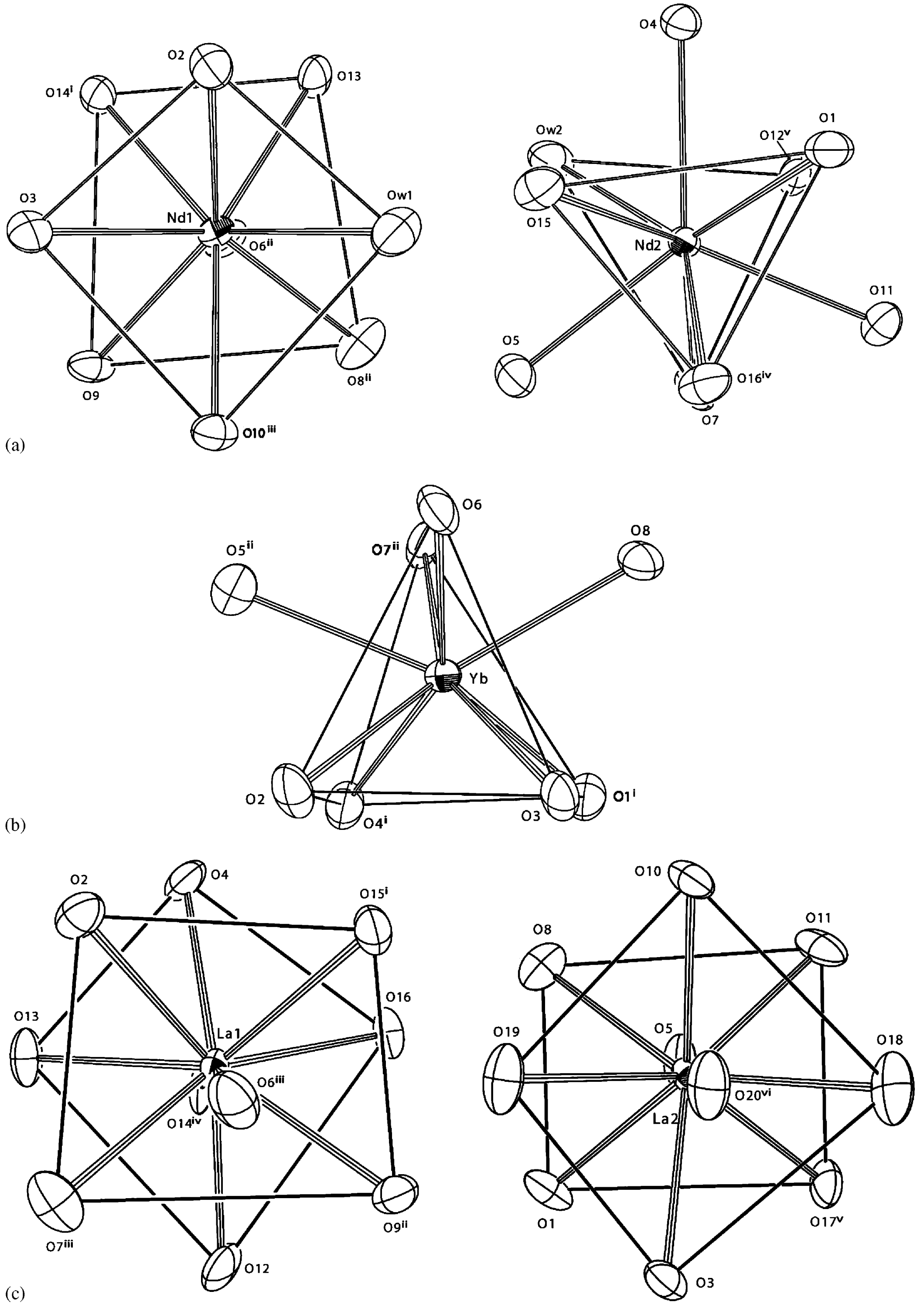

Fig. 3. Representation of the lanthanide polyhedron for **I** to **III**: (a) Nd1 and Nd2 for **I**, the symmetry codes are given in Table 3; (b) Yb for **II**, the symmetry codes are given in Table 5; (c) La1 and La2 for **III**, the symmetry codes are given in Table 7.

into the [100] direction (Fig. 1b). So the structure becomes 3D. Two adjacent, oxalate sharing helices turn in opposite sense. Some free water molecules are localized into the space of these helices.

Another 12-membered elliptic channel (5.5 Å × 11.4 Å), containing the 1,2DAP cation and the crystallization water molecules is running along the [001] direction (Fig. 2). The repetition of these channels, along the plane (001), leads to a 3D distorted honey-comb. All the channels intersect partially thus leading to a very open structure. The free or bound water molecules, as well as the protonated amine, form hydrogen bonding between themselves or with the oxalate oxygen atoms thus strengthening these guest species to the frame (Table 3).

Both Nd atoms are nine-coordinated, with eight oxalate oxygen atoms and one water molecule. The average distances are roughly the same, 2.493 and 2.496 Å for Nd1 and Nd2, respectively (Table 3). However their coordination polyhedra differ [41]. For Nd1, it can be represented as a distorted monocapped square antiprism, with O6^{ii}, the longest distance from Nd1, as a cap (Fig. 3a). For Nd2, the best representation is a distorted tricapped trigonal prism, again the three cap positions (O4, O5 an O11) are the more distant from Nd2 (Fig. 3a, Table 3).

Only two oxalates are non-centrosymmetric, they are planar within 0.043(2) Å. The C–O, C–C distances and the corresponding angles of all the oxalate units are in the expected range for this type of bonding (Table 3) [17–36,42–46]. For the diprotonated amine, the distance C9–C10 is relatively short (1.36(1) Å, Table 3). This value differs from those currently observed in the literature data where C–C and C–N distances are in the range 1.50–1.53 Å and 1.48–1.51 Å, respectively [47–49]. No possible explanation for such a shortening of this distance C9–C10 has been found:

$(C_3N_2H_{12})[Yb(C_2O_4)_2]_2 \cdot 5H_2O$ **II**.

It crystallizes in the orthorhombic system, space group *F*2*dd* (Table 1). The asymmetric unit contains 19 non-hydrogen atoms of which 13 belong to the framework (Table 4). Within the 3D frame, there was one ytterbium and two independent bischelating oxalate groups.

Table 4
Final least-squares atomic parameters with estimated standard deviations for $(C_3N_2H_{12})[Yb(C_2O_4)_2]_2 \cdot 5H_2O$ **II**

Atoms	*x*	*y*	*z*	Ueq. (Å)^2
Yb	0.88978(8)	0.23160(2)	0.064067(7)	0.01453(7)
O1	0.5608(5)	0.3331(3)	−0.0217(2)	0.026(1)
O2	0.7215(6)	0.3167(3)	0.0308(2)	0.029(1)
O3	0.7384(5)	0.1562(3)	0.0158(1)	0.023(1)
O4	0.5545(5)	0.1702(3)	−0.0327(2)	0.028(1)
O5	0.5896(4)	0.1027(3)	0.1480(1)	0.023(1)
O6	0.6911(5)	0.1977(3)	0.1065(1)	0.027(1)
O7	0.8191(5)	0.0002(3)	0.1332(1)	0.025(1)
O8	0.9209(4)	0.0963(3)	0.0903(1)	0.022(1)
C1	0.642(1)	0.2897(4)	0.0018(2)	0.020(1)
C2	0.646(1)	0.1963(4)	−0.0060(2)	0.020(1)
C3	0.6886(6)	0.1297(4)	0.1241(2)	0.019(1)
C4	0.8215(7)	0.0700(4)	0.1151(2)	0.018(1)
N	0.4408(7)	0.2446(4)	0.2022(2)	0.042(2)
C5	0.570(1)	0.2709(6)	0.2282(3)	0.047(2)
C6	0.720(2)	0.267(1)	0.2056(5)	0.040(4)
Ow1	0.909(1)	0	0	0.051(2)
Ow2	0.390(4)	0.2313(6)	0.0611(3)	0.102(2)
Ow3	0.254(1)	0.0991(7)	0.1199(3)	0.092(2)

The ytterbium atom is linked to four oxalate groups and the distances Yb–Yb through these oxalates are homogenous, from 6.0430(3) Å (via Ox1) to 6.0574(4) Å (via Ox2). The connectivity between ytterbium atoms and oxalate ligands results in the formation of a frame containing either 8- or 12-membered channels (Fig. 4a). As for compound **I**, such 8-membered channels are given by helices spreading along the $[\bar{1}\bar{1}0]$ direction (Fig. 4b), leading to the three-dimensionality. Again, two adjacent helices, sharing an oxalate unit, turn in an opposite sense. The 8-membered channels contain only crystallization water molecules while 12-membered channels (5.3 Å × 9.9 Å) contain the same species and also the protonated amine at the borderline.

Another 12-membered elliptic channel (5.2 Å × 9.5 Å) is occurring along the [100] axis (Fig. 5). It contains, in its center, the free water molecule, Ow1, which is localized on a 2-fold axis and one 1,2DAP cation per 12-membered ring. The other water molecules, Ow2 and Ow3, are located at the levels of the Yb polyhedron or of the center of Ox2, respectively. The water molecules and diprotonated amine are bound to the oxygen atoms of the frame by hydrogen bonds or by Van der Waals interactions.

The ytterbium atom is eight-coordinated, with all the oxygen atoms of Ox1 and Ox2. Its bond distances are in the range 2.282(5) Å–2.382(5) Å (average 2.331 Å) (Table 5) and are normal for such lanthanide. The coordination polyhedron can be represented as a distorted dicapped trigonal prism, with O8 and O5 as the cap positions (Fig. 3b). A dihedral angle of 9.73(5)° is observed between the bases of the prism.

Both oxalate units are non-centrosymmetric and Ox1 is less planar than Ox2 (0.052(6) Å versus 0.008(3) Å). The C–O and C–C distances are normal for this type of bonding (Table 5) [17–36,42–46]. Though the amine was disordered, its C–N and C–C distances and the corresponding angles are in expected range [47–49]:

$(C_3N_2H_{12})_2[La_2(C_2O_4)_5] \cdot 5H_2O$ **III**.

This compound crystallizes in the triclinic system, space group P-1. There are two independent lanthanum atoms, five oxalate ligands (Ox1–Ox7, the four last being located at the center symmetry), two diprotonated 1,3-diaminopropane and five water molecules (Table 6). As previously seen for **I** and **II**, all the oxalates are only bischelating. The 3D network is built up by the connectivity of the two lanthanum atoms and the oxalate units.

Instead of three or four oxalate ligands surrounding the lanthanide element which is the usual case, both lanthanum atoms of **III** are linked to five oxalate ligands, in only a chelating way (Fig. 6). To our knowledge, it is the first time that such a lanthanide is bound to five oxalates. This is

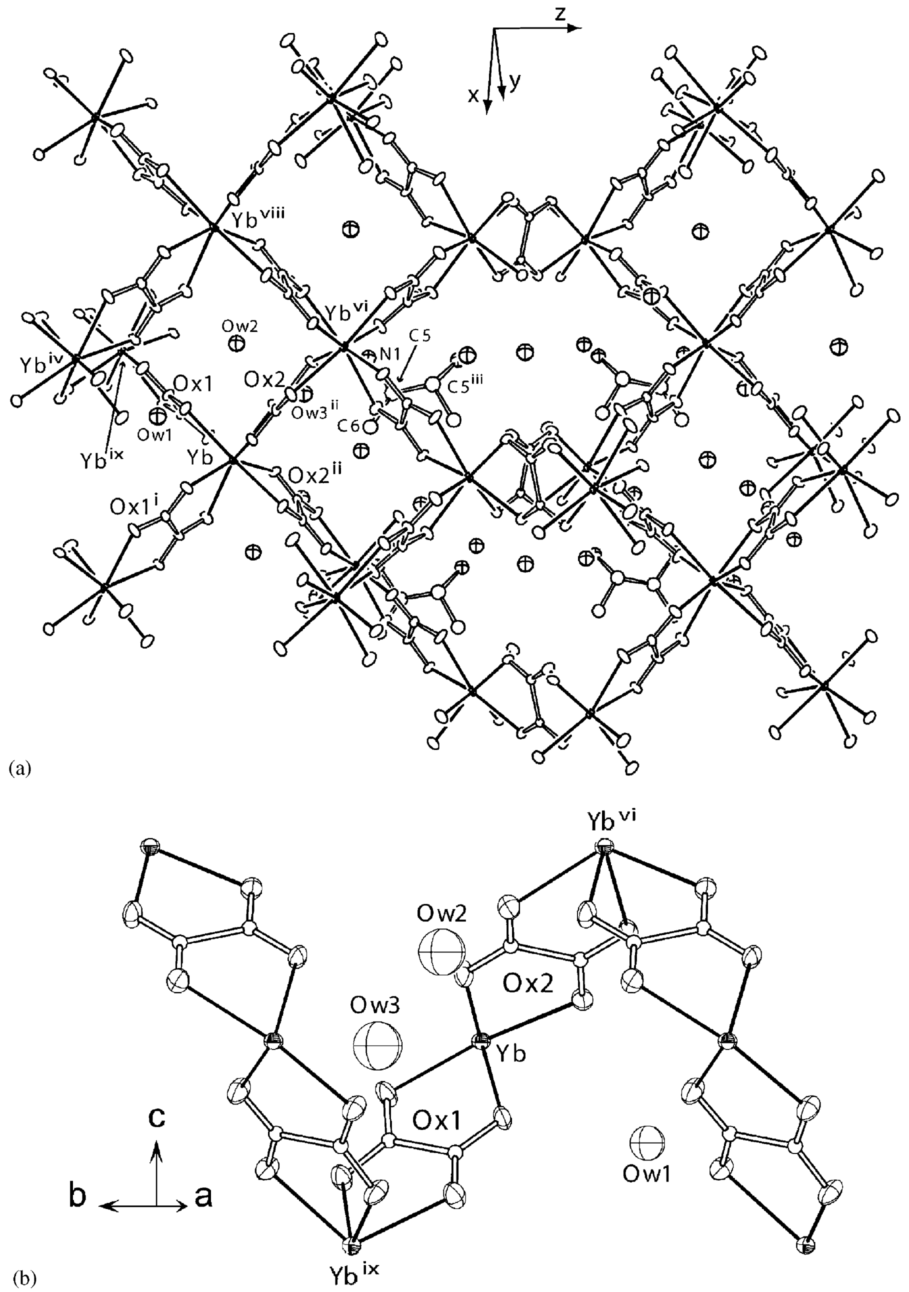

Fig. 4. (a) View onto the $(1\bar{1}0)$ plane of the three-dimensional structure of **II**, showing the 8-membered and the 12-membered channels; (b) view of an helix running along the $[\bar{1}\bar{1}0]$ direction (for clarity reason, only the oxygen atoms involved in the helix formation and the free water molecules are drawn). Thermal ellipsoids are represented at 30% probability. The symmetry codes are given in Table 5.

likely possible, considering the ionic radius of lanthanum which is the highest of the lanthanide series [50,51].

The stacking of the units, presented in Fig. 6, leads to the formation of 12-membered ring, towards the plane (111), which is a quite regular hexagon (Fig. 7a). The edges and angles of such a hexagon, schematized into Fig. 7b, are in the range 6.546(1) Å (via Ox5)–6.806(1) Å (via Ox7) and 118.72(1)–122.22(1)°. Nearly circular channels (9.1 Å × 9.5 Å) are running along the [111] direction. They contain the amine ions and the water molecules, two 1,3DAP ions per one 12-membered ring. The stacking of these hexagons leads to a quite perfect honey-comb layer (Fig. 7c). Note that, within the layer, the two amine cations are alternatively distributed, one horizontal line contains the first (N1–N2) cation and the other the (N3–N4) cation.

These layers are pillared or cross-linked by Ox1 and Ox3 alternatively, leading to roughly three types of 8-membered channels which are at nearby 60° between them. The shape and the size of such channels is slightly variable

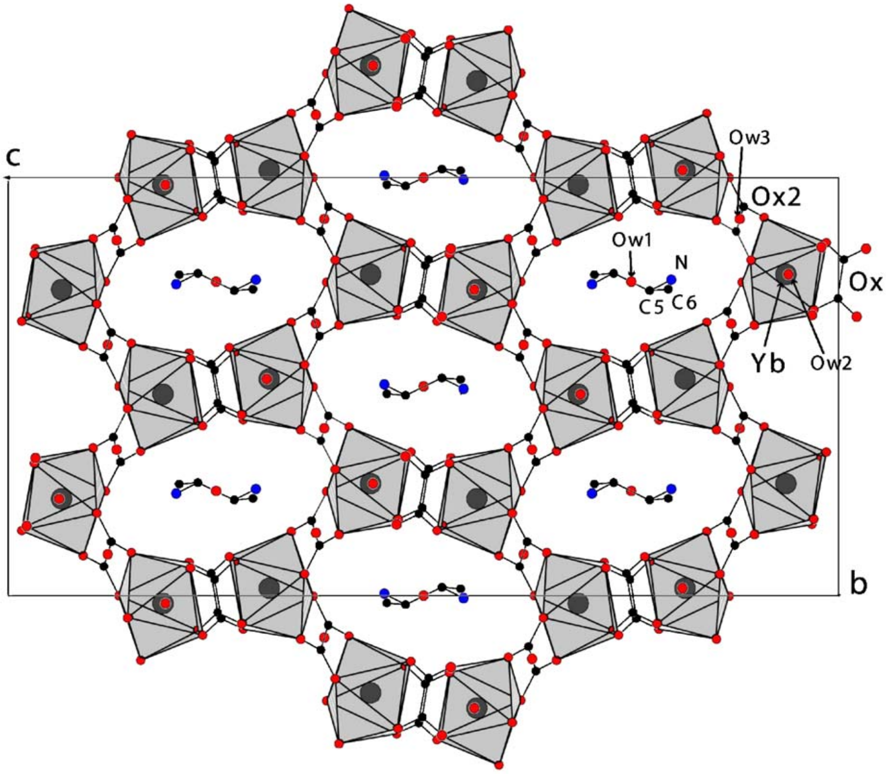

Fig. 5. Projection of the 12-membered channels running in the [001] direction and leading to a 3D distorted honey-comb, for **II**.

but it is less than the one of the 12-membered channel. Along [100] direction, there are two slightly different channels: the one containing the first amine cation is equal to 4.1 Å × 7.1 Å and the one containing the second amine cation is equal to 5.7 Å × 6.5 Å (Fig. 8). In the other directions $[\bar{1}\bar{1}1]$ and $[1\bar{1}1]$ two channels, only one per direction, are observed: 4.0 Å × 6.5 Å and 4.5 Å × 5.9 Å, respectively. So the structure of this compound consists of an open framework.

Both lanthanum atoms are 10-fold coordinated with the oxalate oxygen atoms. The La1–O distance distribution (from 2.570(5) Å to 2.646(6) Å, $\Delta = 0.076$ Å) is narrower than La2–O one (from 2.549(5) Å to 2.696(6) Å, $\Delta = 0.147$ Å). However the two lanthanums present the same average (2.62(2) Å). In both cases, the coordination polyhedron can be described as a dicapped square antiprism (Fig. 3c). For La1, the cap positions are occupied by $O6^{iii}$ and $O14^{iv}$ which are the more distant atoms from La1; a dihedral angle of 8.4(2)° is observed between the two distorted square faces. For La2, O5 and $O20^{vi}$ that are among the more distant atoms from La2 occupy the cap positions and a dihedral angle of 4.6(3)° is observed between the two distorted square faces.

Among the seven oxalate ligands, only three are non-centrosymmetric. Their deviations from planarity are variable, 0.043(4), 0.061(4) and 0.160(4) Å for Ox1, Ox2 and Ox3, respectively. Within the more distorted oxalate, the torsion angle around C5–C6 reaches 17.2(8)° compared to 4.7(7)° for Ox1. However, the bonds lengths and angles are normal for all these oxalates (Table 7).

The distances C–C and C–N of the two amine ions are normal [47–49,52], except for the high C16-N4 = 1.68(2) Å. Such a lengthening of this bond is probably the consequence that N4 interacts four times with the oxygen atoms of the oxalates and Ow2. These Van der Waals interactions are relatively short for a nitrogen atom (from 2.79(1) Å to 3.06(1) Å, Table 7). Although the hydrogen atoms were not localized at all, there are some possible interactions between the other nitrogen atoms, as well as the free water molecules, and the oxygen atoms of the frame.

3.1.1. *Comparison of the structure of compounds **I–III** with some compounds of the literature*

In spite of their differences concerning the number of oxalates surrounding the lanthanide, compounds **I–III** have some similar features: the presence of some 8- or 12-membered rings or channels. Such a presence is usual for the lanthanide-oxalates either 2D or 3D. Some 8-membered channels have been observed many times in mixed *M*-lanthanide oxalates (M = alkaline elements, NH_4^+, etc.) [25–31]. Some 12-membered apertures are already present in the simple layered lanthanide oxalates either decahydrates or hexahydrates [21–24]. The channels can be either produced by a helical arrangement like compounds **I** and **II,** as well as in some papers reported in the literature

Table 5
Selected bond distances (Å) and angles (deg) in $(C_3N_2H_{12})[Yb(C_2O_4)_2]_2 \cdot 5H_2O$ **II**

Yb-O1^{i}	2.282(5)	Yb–O5^{ii}	2.347(5)	
Yb–O6	2.284(4)	Yb–O8	2.359(4)	
Yb–O2	2.286(5)	Yb–O4^{i}	2.373(5)	
Yb–O7^{ii}	2.337(5)	Yb–O3	2.382(5)	
O1–C1	1.254(9)	O1–C1–O2	125.2(7)	
O2–C1	1.245(9)	O1–C1–C2	117.6(5)	
O3–C2	1.256(9)	O2–C1–C2	117.2(6)	Ox1
O4–C2	1.249(9)	O3–C2–O4	128.8(6)	
C1–C2	1.531(9)	O3–C2–C1	115.5(5)	
		O4–C2–C1	115.6(5)	
O5–C3	1.242(7)	O5–C3–O6	127.5(6)	
O6–C3	1.236(8)	O5–C3–C4	115.4(6)	
O7–C4	1.269(8)	O6–C3–C4	117.2(5)	Ox2
O8–C4	1.257(7)	O7–C4–O8	127.1(6)	
C3–C4	1.543(8)	O7–C4–C3	117.2(5)	
		O8–C4–C3	115.7(5)	
N–C5	1.47(1)	N–C5–C6	113.0(9)	
C5–C5^{iii}	1.56(2)	N–C5–C5^{iii}	112.7(6)	
C5–C6	1.51(2)	C6–C5–C5^{iii}	114.6(8)	
Ow1–H1	0.931	H1–Ow1–H1^{iv}	104.8	

Hydrogen bonds and Van der Waals interactions

	D–H	A–H	A–D	D–H–A
Ow1–H1–O3	0.93	2.06	2.981(7)	168.1
N–Ha–Ow1^{v}	0.92	2.00	2.915(11)	176.6
N–Hc–Ow3^{ii}	0.90	2.06	2.924(12)	159.1
N–Hb–O2^{vi}	1.00	2.09	2.937(9)	141.8
Ow2–O6			3.07(3)	
Ow2–Ow3^{ii}			3.09(3)	
Ow3–O7^{vii}			2.93(1)	
Ow3–O6^{vi}			3.04(1)	

Symmetry codes: (i) $x+1/2, -y+1/2, -z$; (ii) $x+1/4, y+1/4, -z+1/4$; (iii) $x, -y+1/2, -z+1/2$; (iv) $x, -y, -z$; (v) $x-3/4, -y+1/4, z+1/4$; (vi) $x-1/4, y-1/4, -z+1/4$; (vii) $x-3/4, y+1/4, -z+1/4$; (viii) $x-1/2, y-1/2, -z$; (ix) $x-1/2, -y-1/2, -z$.

Table 6
Final least-squares atomic parameters with estimated standard deviations for $(C_3N_2H_{12})_2[La_2(C_2O_4)_5] \cdot 5H_2O$ **III**

Atoms	x	y	z	$U_{eq.}$ (Å)^2
La1	−0.25002(4)	0.08746(4)	−0.07496(3)	0.0175(1)
La2	0.25888(4)	0.59055(4)	0.42086(3)	0.0165(1)
O1	0.0943(6)	0.5019(5)	0.2004(5)	0.035(1)
O2	−0.0867(6)	0.3369(5)	0.0397(5)	0.030(1)
O3	0.0900(6)	0.3368(5)	0.3065(4)	0.028(1)
O4	−0.1024(6)	0.1746(5)	0.1495(4)	0.032(1)
O5	0.3777(6)	0.6932(6)	0.3038(5)	0.035(1)
O6	0.3530(6)	0.7795(6)	0.1706(5)	0.034(1)
O7	0.1746(7)	0.8393(6)	0.2254(5)	0.037(1)
O8	0.2187(7)	0.7750(6)	0.3705(5)	0.033(1)
O9	0.4868(6)	0.9463(6)	0.7764(5)	0.034(1)
O10	0.3223(6)	0.7749(5)	0.6092(5)	0.030(1)
O11	0.5188(6)	0.7602(6)	0.5499(5)	0.037(1)
O12	0.6746(6)	0.8884(6)	0.7362(5)	0.038(1)
O13	0.0038(6)	0.1369(6)	−0.0278(5)	0.032(1)
O14	0.1714(6)	0.0852(5)	0.0332(5)	0.032(1)
O15	−0.6113(6)	−0.1580(5)	−0.0199(5)	0.030(1)
O16	−0.4017(6)	−0.0797(6)	−0.0137(5)	0.029(1)
O17	0.6030(6)	0.5215(6)	0.6395(5)	0.033(1)
O18	0.4007(7)	0.5197(7)	0.5703(5)	0.044(2)
O19	0.0187(6)	0.5594(6)	0.3960(5)	0.039(1)
O20	−0.1532(6)	0.5066(6)	0.4468(5)	0.036(1)
C1	0.0011(8)	0.3845(8)	0.1428(7)	0.021(2)
C2	−0.0050(8)	0.2907(8)	0.2043(7)	0.023(2)
C3	0.3294(8)	0.7509(7)	0.2494(7)	0.021(2)
C4	0.2329(9)	0.7920(8)	0.2852(7)	0.024(2)
C5	0.4455(8)	0.8537(8)	0.6813(7)	0.022(2)
C6	0.5562(9)	0.8326(8)	0.6537(7)	0.026(2)
C7	0.0509(8)	0.0637(8)	0.0012(6)	0.021(2)
C8	−0.5027(8)	−0.0684(8)	−0.0093(6)	0.020(2)
C9	0.5009(8)	0.5116(8)	0.5602(7)	0.026(2)
C10	−0.0380(8)	0.5199(8)	0.4560(7)	0.027(2)
N1	0.4106(9)	0.3418(8)	0.1509(7)	0.045(2)
C11	0.432(2)	0.388(2)	0.058(1)	0.103(5)
C12	0.286(1)	0.361(1)	−0.031(1)	0.060(3)
C13	0.249(2)	0.461(2)	0.022(1)	0.107(6)
N2	0.110(2)	0.416(1)	−0.069(1)	0.113(5)
N3	0.771(1)	0.051(1)	0.273(1)	0.079(3)
C14	0.961(3)	0.026(2)	0.382(2)	0.143(8)
C15	0.899(2)	0.103(1)	0.380(1)	0.088(4)
C16	1.034(2)	0.034(1)	0.320(1)	0.085(4)
N4	1.183(1)	0.176(1)	0.3871(9)	0.070(3)
Ow1	0.678(1)	0.3935(9)	0.1986(8)	0.084(3)
Ow2	0.592(1)	0.783(1)	0.187(1)	0.118(4)
Ow3	0.929(1)	0.704(1)	0.297(1)	0.111(4)
Ow4	0.716(1)	0.683(1)	0.355(1)	0.127(4)
Ow5	0.680(2)	0.950(1)	0.465(1)	0.137(5)

[20,34,53] or by some layers bridged, in out-of-plane manner by a supplementary oxalate unit [33–36].

The dimensions and geometry of the templates, but also their proportions relative to the frame, can tune the size and the shape of the channels. An example has been given, by comparing the structure of two layered oxalates: the decahydrate $[\{Gd(H_2O)_3\}_2(C_2O_4)_3] \cdot 4H_2O$ [21–24] and $[\{Gd(H_2O)_3\}_2(C_2O_4)_3]$ [17,18]. Considering the free water molecules as a template, the loss of these molecules induces a deep transformation of the ring: the nearly hexagonal ring for the former compound transforms into a rectangular ring for the latter compound. The templates, used here 1,2DAP and 1,3DAP, are quite similar by their size and shape. However, in compounds **I** or **II** to **III**, their ratios per lanthanide atom change. For **I** and **II**, only one amine cation is present in the 12-membered ring (Figs. 2 and 5). Thus, these channels present roughly the same elliptical cross-section, that fits enough with the shape of 1,2DAP. On the opposite, two 1,3DAP cations per 12-membered ring are present for **III** and thus the nearly elliptical section observed for **I** and **II** would change into a larger area, close to a perfect hexagonal ring for **III**.

Although there are few reported organic-templated lanthanide oxalates, these ones are generally 3D with 8- or 12-membered channels, which intersect partially in one or two or three directions. In general, one can compare these compounds to the more-known zeolites.

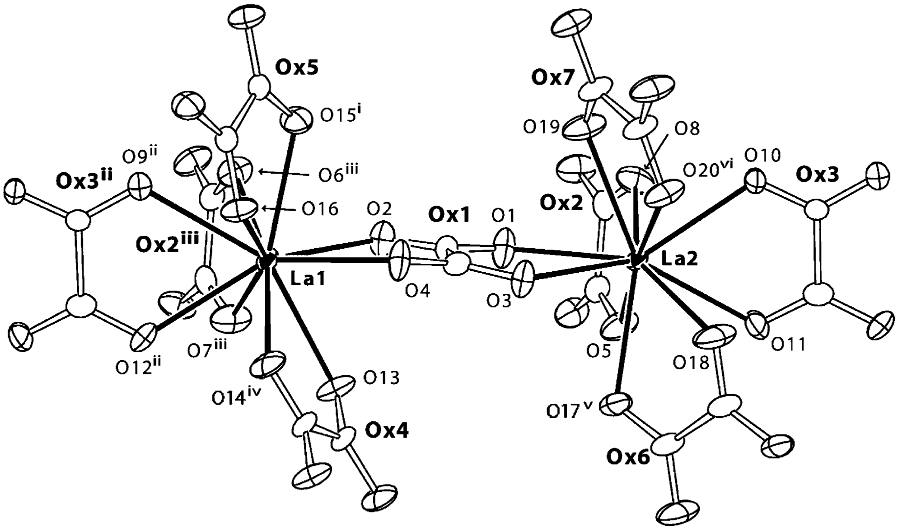

Fig. 6. View of the surroundings of both lanthanum atoms made with five oxalate group per atom. Thermal ellipsoids are represented at 50% probability. The symmetry codes are given in Table 7.

*3.1.2. Extension of compounds **I–III** to some other lanthanide elements and characterization of the observed families*

These compounds were made at reflux (cf. Section 2). Only **I** can extend to some other lanthanide, thus forming a family from cerium to thulium. The cell-constants are reported in Table 8. For the family **I**, *a–c* parameters decrease with the ionic radius of the lanthanide [50,51]. The variation of *a* parameter is small compared to the variations of *b* and *c*. Roughly, the so-called lanthanide contraction and the Vegard rule are approximately respected.

Apart from the oxalate infrared bands (around 1500–1650, 1490, 1315, 1355 and 795 cm^{-1}) which are roughly in the same positions for compound **I**–**III** and which are characteristic of lanthanide oxalates, these spectra exhibit some features relative to amine and to water function [54–56]. In the spectra of **II** and **III**, two broad absorption bands are clearly observed in the 2500–3600 cm^{-1} domain: the first band centered at 3450 cm^{-1} is attributed to stretching vibrations of the water molecules, the second band centered at 3100 cm^{-1}, which is composed to some overlapping bands (3100, 2930, 2700 and 2600 cm^{-1}), is relevant to stretching vibrations of the amine function (νN–H and νC–H). In the spectrum of **I**, these two broad bands also appear but they are quite overlapping. This slight difference is perhaps relevant to the water molecule status: for **I**, there are two types of water molecules, bound to the neodymium and free while for **II** and **III** there are only free water molecules.

Thermogravimetric analyses of the compounds **I**–**III** are presented in Fig. 9. In all the cases the total mass loss agrees quite well with the proposed formula leading to the corresponding sesquioxide: obs. 57.7% (th. 58.28%), 55.3% (54.39%) and 66.6% (66.05%) for **I**–**III**, respectivly. The dehydration process for **I** and **III** occurs in one stage beginning at 50 °C and ending at 150 °C while for **II**, two overlapping stages are noted, 50–150 °C (roughly $3H_2O$) and 150 °C–250 °C (roughly $2H_2O$). Then a well-defined plateau, corresponding to the corresponding anhydrous compound is observed up to 300 or 320 °C for **I**, **III** or **II**, respectively. Beyond these temperatures and up to practically 400 °C the mass loss is very steep, then it slows down between 400 and 800 °C.

For **III**, the curve is quite similar to the one of lanthanum oxalate decahydrate, while for **I** and **II**, there are some inflexion or singular points which are absent from the decomposition of the simple corresponding oxalates either decahydrate or hexahydrate [57–61]. At these points, the remaining solid materials could have the composition represented in the respective curves (Fig. 9). In the same way between 500 and 700 °C, the presence of $Nd_2(CO_3)_2O$ in **I** or the presence of the non-stoichiometric dioxycarbonate diytterbium (x~0.3) in **II** do not occur through the decomposition of the corresponding lanthanide oxalate alone.

For **I**–**III**, the onset of the decomposition, at 300 or 320 °C, is marked by a slight endothermic effect immediately followed by a strong exothermic effect (unrepresented). This endothermic peak would be due to the partial amine departure immediately followed by an oxalate decomposition which is, in the used conditions (O_2), strongly exothermic. For **I** and **II**, it is likely that the departure of the amine and consequently of a partial departure of the oxalate ligand induces an activation energy which modifies strongly the thermal behavior of these compounds leading to various materials

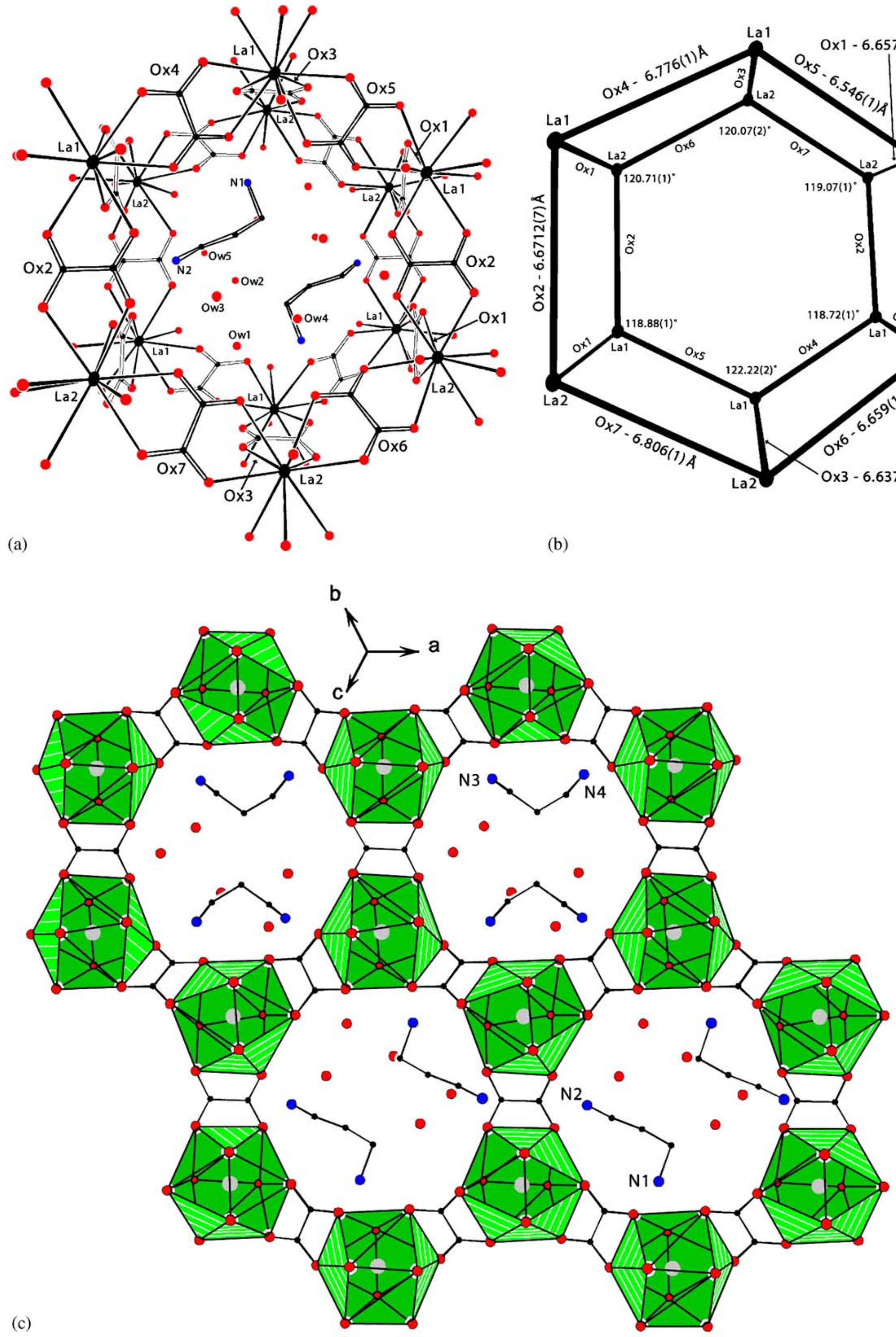

Fig. 7. View along the [111] direction, for **III**: (a) of 12-membered hexagons; (b) schematization of these hexagons showing the La–La distances and the corresponding angles; (c) of the packing of these hexagons leading to 3D honey-comb whose channels contain the guest species.

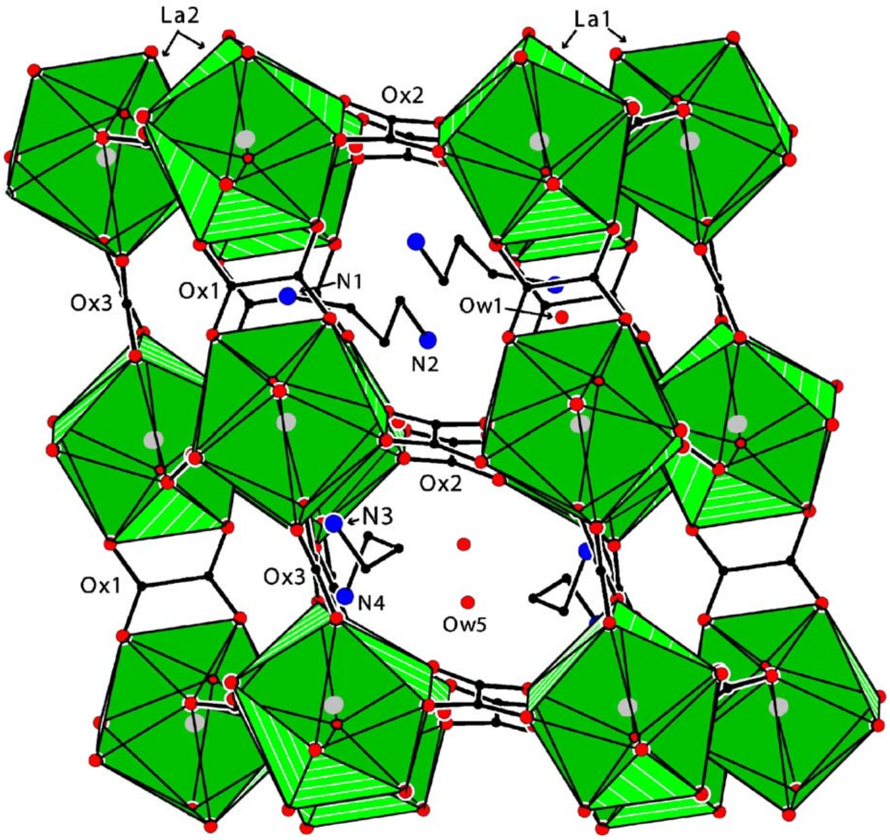

Fig. 8. View along the [100] direction of the two 8-membered channel for **III**.

which were present at these singular points and which were not observed so clearly in the literature data [57–61].

At last, trying to exchange the H_2O by D_2O molecules of these compounds, **I–III**, between 100 and 250 °C were unsuccessful (see experimental technique in Ref. [34]). So the dehydration process is irreversible. Such an irreversible process is in agreement with the data obtained by the TGA of these compounds between 100 and 250 °C under atmospheric air. It is likely that the pores are obstructed by the presence of diprotonated amine. However, as shown by the X-ray powder of these compounds heated at different temperature, **II** and **III** are crystalline up to 250 °C while an amorphous state is observed for **I** at 150 °C. In **II** and **III,** there are only free water molecules and so the frame stays unaffected by the water loss while, in **I**, some water molecules (Ow1 and Ow2) belong to close environment of the neodymium atoms and their losses, at 150 °C, lead to an amorphization.

4. Conclusion

The present study shows that 3D open-framework lanthanide oxalate compounds can be synthesized, with mild hydrothermal route, in presence of 1,2 or 1,3-diaminopropane. Furthermore, through these examples it has been shown that the templates can tune the shape and the size of the channels. For **III**, both lanthanum atoms are

Table 7
Bond distances (Å) and angles (deg) in $(C_3N_2H_{12})_2[La_2(C_2O_4)_5]\cdot 5H_2O$ **III**

La1–O2	2.570(5)	La2–O10	2.549(5)	
La1–O15^{i}	2.573(6)	La2–O19	2.590(6)	
La1–O12^{ii}	2.603(6)	La2–O1	2.603(5)	
La1–O4	2.609(5)	La2–O8	2.605(5)	
La1–O13	2.628(6)	La2–O11	2.606(6)	
La1–O7^{iii}	2.629(6)	La2–O17^{v}	2.615(6)	
La1–O16	2.632(5)	La2–O3	2.618(5)	
La1–O9^{ii}	2.636(6)	La2–O5	2.625(6)	
La1–O6^{iii}	2.644(6)	La2–O18	2.675(6)	
La1–O14^{iv}	2.646(6)	La2–O20^{vi}	2.696(6)	
O1–C1	1.252(9)	O2–C1–O1	125.8(7)	
O2–C1	1.243(9)	O1–C1–C2	117.3(7)	
O3–C2	1.266(9)	O2–C1–C2	117.0(7)	Ox1
O4–C2	1.256(9)	O4–C2–O3	125.3(7)	
C1–C2	1.54(1)	O3–C2–C1	117.0(7)	
		O4–C2–C1	117.8(7)	
O5–C3	1.259(9)	O5–C3–O6	127.1(8)	
O6–C3	1.252(9)	O5–C3–C4	116.0(7)	
O7–C4	1.253(9)	O6–C3–C4	116.9(7)	Ox2
O8–C4	1.244(9)	O7–C4–O8	125.7(8)	
C3–C4	1.53(1)	O7–C4–C3	116.9(7)	
		O8–C4–C3	117.4(7)	
O9–C5	1.253(9)	O9–C5–O10	125.8(7)	
O10–C5	1.255(9)	O9–C5–C6	116.6(7)	
O11–C6	1.256(9)	O10–C5–C6	117.6(7)	Ox3
O12–C6	1.25(1)	O11–C6–O12	126.3(8)	
C5–C6	1.53(1)	O11–C6–C5	116.5(7)	
		O12–C6–C5	117.3(7)	

Table 7 (*continued*)

O13–C7	1.262(8)	O13–C7–O14	126.4(7)	
O14–C7	1.237(9)	O13–C7–C7$^{\text{iv}}$	116.8(8)	Ox4
C7–C7$^{\text{iv}}$	1.54(2)	O14–C7–C7$^{\text{iv}}$	116.8(8)	
O15–C8	1.266(9)	O15–C8–O16	126.4(7)	
O16–C8	1.251(9)	O15–C8–C8$^{\text{i}}$	116.0(9)	Ox5
C8–C8$^{\text{i}}$	1.56(2)	O16–C8–C8$^{\text{i}}$	117.6(9)	
O17–C9	1.259(9)	O17–C9–O18	126.0(7)	
O18–C9	1.252(9)	O17–C9–C9$^{\text{v}}$	117.3(9)	Ox6
C9–C9$^{\text{v}}$	1.54(2)	O18–C9–C9$^{\text{v}}$	116.7(8)	
O19–C10	1.257(9)	O19–C10–O20	125.9(7)	
O20–C10	1.256(9)	O19–C10–C10$^{\text{vi}}$	116.5(9)	Ox7
C10–C10$^{\text{vi}}$	1.52(2)	O20–C10–C10$^{\text{vi}}$	117.5(9)	
N1–C11	1.52(2)	N1–C11–C12	107(1)	
C11–C12	1.59(2)	C11–C12–C13	110(1)	
C12–C13	1.50(2)	N2–C13–C12	102(1)	
C13–N2	1.49(2)			
N3–C15	1.47(2)	N3–C15–C14	115(1)	
C14–C16	1.35(3)	C16–C14–C15	114(2)	
C14–C15	1.36(2)	N4–C16–C14	113(1)	
C16–N4	1.68(2)			
Possible hydrogen bonds and Van der Waals interactions				
N1–O14	2.88(1)	Ow1–N1	2.78(1)	
N1–O17$^{\text{v}}$	2.92(1)	Ow1–O15$^{\text{iv}}$	2.83(1)	
N1–O16$^{\text{iv}}$	3.14(1)	Ow2–O6	2.71(1)	
N2–O2$^{\text{iii}}$	3.00(1)	Ow2–N3$^{\text{ix}}$	2.79(2)	
N2–O2	3.07(2)	Ow2–Ow4$^{\text{v}}$	2.99(2)	
N2–O1$^{\text{iii}}$	3.10(2)	Ow3–O19$^{\text{vii}}$	2.71(1)	
N3–O4$^{\text{vii}}$	2.86(1)	Ow3–Ow4	2.77(2)	
N3–O9$^{\text{v}}$	2.89(1)	Ow3–N2$^{\text{iv}}$	2.80(2)	
N3–O10$^{\text{v}}$	3.00(1)	Ow3–O8$^{\text{vii}}$	2.92(1)	
N4–O3$^{\text{vii}}$	2.79(1)	Ow4–N4$^{\text{viii}}$	3.00(2)	
N4–O12$^{\text{viii}}$	2.83(1)	Ow4–O18$^{\text{v}}$	2.90(1)	
N4–O11$^{\text{viii}}$	3.06(1)	Ow5–O8$^{\text{xi}}$	2.98(1)	
O18–O20$^{\text{vi}}$	2.719(9)	Ow5–O11$^{\text{x}}$	3.07(2)	

Symmetry codes: (i) $-x-1, -y, -z$; (ii) $x-1, y-1, z-1$; (iii) $-x, -y+1, -z$; (iv) $-x, -y, -z$; (v) $1-x, 1-y, 1-z$; (vi) $-x, 1-y, 1-z$; (vii) $x+1, y, z$; (viii) $-x+2, -y+1, -z+1$; (ix) $x, y+1, z$; (x) $-x+1, -y+1, -z$; (xi) $-x+1, -y+2, -z+1$.

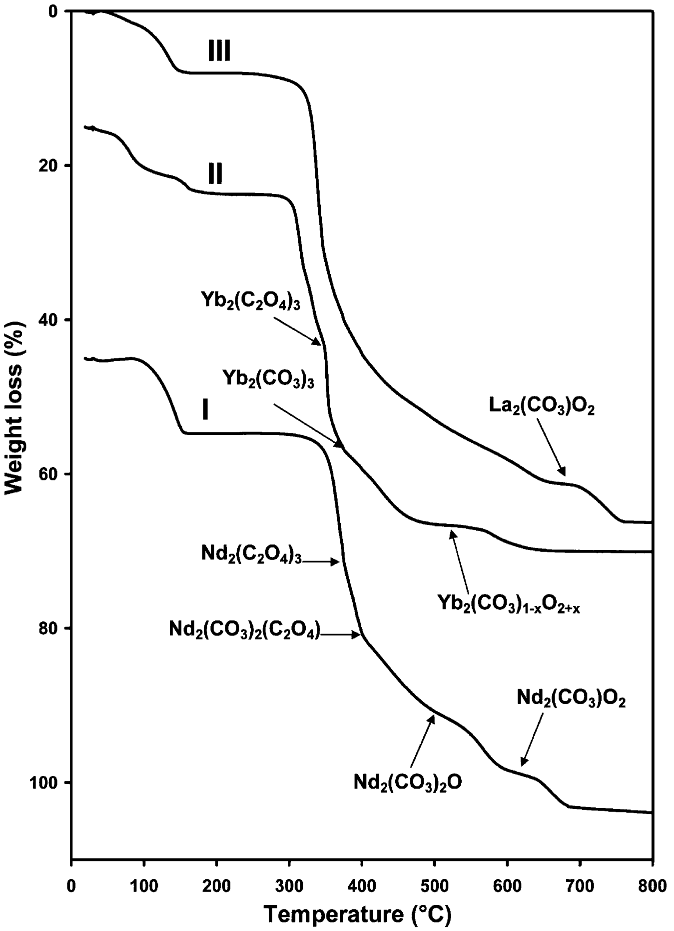

Fig. 9. TGA curves, between 20 and 800 °C, of the compounds **I**–**III**. The **II** and **I** curves are shifted, over the *Y*-axis, by 15% and 45%, respectively.

Table 8
Cell constants of the $(C_3N_2H_{12})[Ln(H_2O)(C_2O_4)_2]_2 \cdot 3H_2O$ **I**, according to the ionic radius of the lanthanide

Ln	r_{Ln}*	a (Å)	b (Å)	c (Å)	α (deg)	β (deg)	γ (deg)	V (Å)^3
Ce	1.196	7.821(5)	11.997(6)	13.102(5)	93.14(7)	94.20(7)	108.12(5)	1161(1)
Pr	1.179	7.815(4)	11.945(4)	12.995(4)	93.14(5)	94.06(5)	108.17(4)	1145.9(8)
Nd	1.163	7.813(3)	11.926(3)	12.990(3)	93.14(4)	93.93(3)	108.76(2)	1139.6(6)
Sm	1.132	7.790(3)	11.802(4)	12.899(3)	93.26(5)	93.63(4)	108.97(4)	1115.5(6)
Eu	1.120	7.795(3)	11.758(4)	12.853(3)	93.24(4)	93.52(3)	109.07(3)	1107.6(6)
Gd	1.107	7.781(3)	11.703(4)	12.820(3)	93.36(5)	93.32(4)	109.14(3)	1097.3(6)
Tb	1.095	7.781(2)	11.646(3)	12.798(4)	93.38(3)	93.05(3)	109.21(2)	1090.0(5)
Dy	1.083	7.765(3)	11.561(4)	12.732(4)	93.37(3)	92.82(3)	109.09(3)	1075.4(7)
Y	1.075	7.786(3)	11.551(3)	12.731(2)	93.30(3)	92.60(3)	109.50(3)	1075.0(5)
Ho	1.072	7.775(5)	11.551(6)	12.720(4)	93.25(3)	92.74(6)	109.46(3)	1072.7(9)
Er	1.062	7.775(2)	11.501(3)	12.695(2)	93.37(3)	92.56(3)	109.57(3)	1065.3(4)
Tm	1.052	7.781(5)	11.444(6)	12.683(3)	93.56(5)	92.25(4)	109.52(6)	1060.2(9)

The lanthanide ionic radius are those with a 9-coordination number [50].

surrounded by five chelating oxalate units and that is original.

The supplementary materials has been sent to the Cambridge Crystallographic Data Centre, 12 union road, Cambridge CB2 1EZ UK, under the numbers, CCDC 266703, CCDC 266704 and CCDC 266705 for **I–III**, respectively.

Acknowledgments

Thanks are also due to Rhodia for the free furniture of some salts of lanthanide.

References

[1] F. Serpaggi, G. Férey, J. Mater. Chem. 8 (1998) 2737–2741.
[2] S.R. Batten, R. Robson, Angew Chem. Int. Ed. 37 (1998) 1460–1494.
[3] T. Chirayil, P.Y. Zavalij, S. Whittingham, Chem. Mater. 10 (1998) 2629–2640.
[4] S. Ayyappan, A.K. Cheetham, S. Natarajan, C.N.R. Rao, Chem. Mater. 10 (1998) 3746–3755.
[5] H. Li, M. Eddaoudi, M. O'Keeffe, O.M. Yaghi, Nature 402 (1999) 276–279.
[6] A.K. Cheetham, G. Férey, T. Loiseau, Angew. Chem. Int. Ed. 38 (1999) 3268–3292.
[7] T.M. Reineke, M. Eddaoudi, M. O'Keeffe, O.M. Yaghi, Angew. Chem. Int. Ed. 38 (1999) 2549–2593.
[8] P.J. Hagrman, D. Hagrman, J. Zubieta, Angew. Chem. Int. Ed. 38 (1999) 2638–2684.
[9] T.M. Reineke, M. Eddaoudi, M. Fehr, D. Kelley, O. M Yaghi, J. Am. Chem. Soc. 121 (1999) 1651–1657.
[10] G. Férey, J. Solid State Chem. 152 (2000) 37–48.
[11] A. Choudhury, S. Natarajan, C.N.R. Rao, Chem. Eur. J. 6 (2000) 1168–1175.
[12] M. O'Keeffe, M. Eddaoudi, H. Li, M. Reineke, O.M. Yaghi, J. Solid State Chem. 152 (2000) 3–20.
[13] G. Férey, Chem. Mater. 13 (2001) 3084–3098.
[14] P.J. Hagrman, R. Finn, J. Zubieta, Solid State Sci. 3 (2001) 745–774.
[15] J.L.C. Rowsell, O.M. Yaghi, Micropor. Mesopor. Mater. 73 (2004) 3–14.
[16] C.N.R. Rao, Angew. Chem. Int. Ed. 43 (2004) 1466–1496.
[17] D. Trollet, S. Roméro, A. Mosset, J.C. Trombe, C. R. Acad. Sci. Paris IIb 325 (1997) 663–670.
[18] D. Trollet, S. Roméro, A. Mosset, J.C. Trombe, Polyhedron 17 (1998) 3977–3978.
[19] J.C. Trombe, J. Jaud, J. Chem. Crystallogr. 33 (2003) 19–26.
[20] M. Camara, C. Daiguebonne, K. Boubekeur, T. Roisnel, Y. Gérault, C. Baux, F. Le Dret, O. Guillou, C. R. Chimie 6 (2003) 405–415.
[21] W. Ollendorf, F. Weigel, Inorg. Nucl. Chem. Lett. 5 (1969) 263–269.
[22] A. Michaelides, S. Soulika, A. Aubry, Mater. Res. Bull. 23 (1988) 579–585.
[23] B. Beagley, R.G. Pritchard, N.P. Evmiridis, A. Michailides, S. Soulika, Acta Crystallogr. C 44 (1988) 174–175.
[24] E. Hansson, Acta Chem. Scand. 24 (1970) 2969–2982;
E. Hansson, Acta Chem. Scand. 26 (1972) 1337–1350;
E. Hansson, Acta Chem. Scand. 27 (1973) 823–834.
[25] T.R.R. McDonald, J.M. Spink, Acta Crystallogr. 23 (1967) 944–949.
[26] T. Bataille, D. Louër, Acta Crystallogr. C 55 (1999) 1760–1762.
[27] T. Bataille, M. Louër, J.-P. Auffrédic, D. Louër, J. Solid State Chem. 150 (2000) 81–95.
[28] T. Bataille, J.-P. Auffrédic, D. Louër, J. Mater. Chem. 10 (2000) 1707–1711.
[29] J.C. Trombe, P. Thomas, C. Brouca-Cabarrecq, Solid State Sci. 3 (2001) 309–319.
[30] S. Roméro, A. Mosset, J.C. Trombe, Eur. J. Solid State Inorg. Chem. 32 (1995) 1053–1063.
[31] T. Bataille, J.-P. Auffrédic, D. Louër, Chem. Mater. 11 (1999) 1559–1567.
[32] F. Fourcade-Cavillou, J.C. Trombe, Solid State Sci. 4 (2002) 1199–1208.
[33] J.C. Trombe, A. Mohanu, C. Brouca-Cabarrecq, Fifth International Conference on f-Elements, Geneva, Switzerland, August 24–29, 2003.
[34] J.C. Trombe, A. Mohanu, Solid State Sci. 6 (2004) 1403–1419.
[35] R. Vaidhyanathan, S. Natarajan, C.N.R. Rao, Chem. Mater. 13 (2001) 185–191.
[36] R. Vaidhyanthan, S. Natarajan, C.N.R. Rao, Inorg. Chem. 41 (2002) 4496–4501.
[37] R.H. Blessing, Acta. Crystallogr. A 51 (1995) 33–38.
[38] A. Altomare, G. Cascarano, C. Giacovazzo, A. Guagliardi, M.C. Burla, G. Polidori, M. Camalli, J. Appl. Crystallogr. 27 (1994) 1045–1050.
[39] G.M. Sheldrick, SHELXL-97, Program for the Refinement of Crystal Structures, University of Göttingen, Germany, 1997.
[40] S. Natarajan, J. Solid State Chem. 148 (1999) 50–55.
[41] M.G.B. Drew, Coordination Chem. Rev. 24 (1977) 179–275.
[42] S. Roméro, A. Mosset, J.C. Trombe, Eur. J. Solid State Chem. 127 (1996) 256–266.
[43] S. Roméro, A. Mosset, J.C. Trombe, Eur. J. Solid State Inorg. Chem. 34 (1997) 209–219.
[44] S. Roméro, J.C. Trombe, Polyhedron 18 (1999) 1653–1659.
[45] J.C. Trombe, S. Roméro, Solid State Sci. 2 (2000) 279–283.
[46] N. Audebrand, E. Jeanneau, T. Bataille, S. Raite, D. Louër, Solid State Sci. 6 (2004) 579–591.
[47] Y. Liu, L. Na, G. Zhu, F.-S. Xiao, W. Pang, R. Xu, J. Solid State Chem. 149 (2000) 107–112.
[48] A. Tuel, V. Gramlichand, Ch. Barlocher, Micropor. Mesopor. Mater. 41 (2000) 217–226.
[49] L. Baouab, A. Jouini, J. Solid State Chem. 141 (1998) 343–351.
[50] R.D. Shannon, Acta Crystallogr. A 32 (1976) 751–767.
[51] Y.Q. Jia, J. Solid State Chem. 95 (1991) 184–187.
[52] N. Simon, N. Guillou, T. Loiseau, F. Taulelle, G. Férey, J. Solid State Chem. 147 (1999) 92–98.
[53] E. Jeanneau, N. Audebrand, D. Louer, Chem. Mater. 14 (2002) 1187–1194.
[54] J. Fujita, A.E. Martell, K. Nakamoto, J. Chem. Phys. 36 (1962) 324.
[55] K. Nakamoto, Infrared Spectra of Inorganic and Coordination Compounds, second ed, Wiley-Interscience, New York, 1963.
[56] N.B. Colthup, L.H. Daly, S.E. Wiberley, Introduction to Infrared and Raman Spectroscopy, Academic Press, New York, 1975.
[57] A. Glassner, M. Steinberg, J. Inorg. Nucl. Chem. 16 (1961) 279–287.
[58] P. Pascal, in: Nouveau Traité de Chimie Minérale, Tome VII, Masson, Paris, 1959, pp. 1006–1012.
[59] M.J. Fuller, J. Pinkstone, J. Less Common Met. 70 (1980) 127–142.
[60] V.V.S. Rao, R.V.G. Rao, A.B. Biswas, J. Inorg. Nucl. Chem. 27 (1965) 2525–2531.
[61] G.L. Jeyaraj, J.E. House Jr., Thermochim. Acta 71 (1983) 345–350.